Since January 2020 Elsevier has created a COVID-19 resource centre with free information in English and Mandarin on the novel coronavirus COVID-19. The COVID-19 resource centre is hosted on Elsevier Connect, the company's public news and information website.

Journal of Virological Methods 201 (2014) 1–6

Contents lists available at ScienceDirect

Journal of Virological Methods

journal homepage: www.elsevier.com/locate/jviromet

Cell adhesion as a novel approach to determining the cellular binding motif on the severe acute respiratory syndrome coronavirus spike protein

Hsin-Hou Chang[a,b], Po-Kong Chen[b], Guan-Ling Lin[b], Chun-Jen Wang[c], Chih-Hsien Liao[a], Yu-Cheng Hsiao[a], Jing-Hua Dong[a], Der-Shan Sun[a,b,*]

[a] Department of Molecular Biology and Human Genetics, Tzu-Chi University, Hualien, Taiwan
[b] Institute of Medical Sciences, Tzu-Chi University, Hualien, Taiwan
[c] The Department of Life Sciences, Tzu-Chi University, Hualien, Taiwan

Article history:
Received 21 August 2013
Received in revised form 20 January 2014
Accepted 24 January 2014
Available online 13 February 2014

Keywords:
SARS-CoV
Spike protein
Vero E6 cells
Binding motif

A B S T R A C T

Emerging life threatening pathogens such as severe acute aspiratory syndrome-coronavirus (SARS-CoV), avian-origin influenzas H7N9, and the Middle East respiratory syndrome coronavirus (MERS-CoV) have caused a high case-fatality rate and psychological effects on society and the economy. Therefore, a simple, rapid, and safe method to investigate a therapeutic approach against these pathogens is required. In this study, a simple, quick, and safe cell adhesion inhibition assay was developed to determine the potential cellular binding site on the SARS-CoV spike protein. Various synthetic peptides covering the potential binding site helped to minimize further the binding motif to 10–25 residues. Following analyses, 2 peptides spanning the 436–445 and 437–461 amino acids of the spike protein were identified as peptide inhibitor or peptide vaccine candidates against SARS-CoV.

1. Introduction

Severe acute respiratory syndrome (SARS) first appeared in Asia in 2002, caused by the SARS-coronavirus (SARS-CoV) (Drosten et al., 2003; Holmes, 2003; Peiris et al., 2003). The illness quickly spread worldwide and affected more than 8000 people with a high case-fatality rate (Kuehn, 2013). Newly emerging pathogens such as the avian influenza A virus H7N9 (Wu and Gao, 2013) and MERS-CoV (Middle East Respiratory syndrome coronavirus, also known as HCoV-EMC) (Kuehn, 2013) are severe public health problems that cause a high case-fatality rate and widespread psychological effects on society and the economy. A simple method is required to investigate a therapeutic approach to these diseases without contacting the biohazardous virus.

Previous studies have completed whole genome sequences (29,751 base pairs) (Marra et al., 2003; Ruan et al., 2003). The data reveal SARS-CoV to be a novel coronavirus that does not belong to any of the 3 known classes of coronavirus (Marra et al., 2003). The genomes encode 23 putative proteins, including known coronavirus proteins such as replicase 1A, replicase 1B, spike glycoprotein (S), small envelope protein, membrane glycoprotein, and nucleocapsid protein (Marra et al., 2003; Ruan et al., 2003). The *S* gene [nucleotide (nt) 21,492–25,259] encodes a transmembrane glycoprotein on the viral surface and is responsible for binding and entry into the host cells (Marra et al., 2003). The S protein can be divided into 2 functional domains: S1 and S2. The S1 domain contains a receptor-binding domain (RBD) responsible for specific binding to the host receptor (Gallagher and Buchmeier, 2001). The angiotensin-converting enzyme 2 (ACE2) is a functional receptor for SARS-CoV (Li et al., 2003). After binding to ACE2, conformational change of the S protein induces exposure of the S2 domain and assists the virus in fusing to the host cells (Matsuyama and Taguchi, 2002). Therefore, the RBD within the S1 domain is the target for development of virus-entry blocking peptides and neutralizing antibodies to prevent SARS-CoV infections. Previous studies have used various methods to investigate the potential RBD from amino acids spanning 303–537 (Xiao et al., 2003), 270–510 (Babcock et al.,

Abbreviations: SARS-CoV, severe acute respiratory syndrome-coronavirus; S, spike; RBD, receptor-binding domain; ACE2, angiotensin-converting enzyme 2; RBM, receptor-binding motif; MTT, 3-(4,5-dimethylthiazol-2-yl)-2,5-diphenyltetrazolium bromide.

* Corresponding author at: Department of Molecular Biology and Human Genetics, Tzu-Chi University, No. 701, Section 3, Zhong-Yang Road, Hualien 970, Taiwan. Tel.: +886 3 8565301x2681; fax: +886 3 8561422.
E-mail addresses: dssun@mail.tcu.edu.tw, dershansun@yahoo.com (D.-S. Sun).

0166-0934
http://dx.doi.org/10.1016/j.jviromet.2014.01.022

2004), 318–510 (He et al., 2004; Wong et al., 2004), 485–625 (Zhou et al., 2004), 261–672 (Sui et al., 2004), 48–358 (Chou et al., 2005), and 450–650 (Zhao et al., 2005), which all span hundreds of residues. A receptor-binding motif (RBM) (residues 424–494) located within the RBD has been identified based on the crystal structure of the SARS-CoV spike protein RBD (residues 306–527) with the receptor ACE2 (Li et al., 2005). However, no effective therapeutic agents against SARS-CoV have been developed in humans (Jiang et al., 2013).

In this study, a cell-adhesion inhibition assay was established to characterize further the potential RBM of the SARS-CoV S protein. Synthetic peptides spanning the potential binding site were used and the RBM was further narrowed to approximately 10–25 residues. This method is useful for characterizing the potential RBM in the RBD of newly emerged coronaviruses in a quick, simple, and safe manner without contacting life threatening pathogens.

2. Materials and methods

2.1. Construction of S1-1/pGEX-6P-3, S1-2/pGEX-6P-1, and S1-3/pGEX-6P-1 expression plasmids

Using 2 plasmids encoding the SARS-CoV spike S1 protein-TW1-#18 [nucleotide (nt) (nt 20,704–22,087)] and TW1-#19 (nt 21,826–22,087) as templates, an S1-1 encoding SARS-CoV S protein 1–446 amino acid was produced and amplified by polymerase chain reaction (PCR), using one pair of primers: SS-F1-2 containing the *Eco*RI site (5′-GGAATTCCATGTTTATTTTCTTATTATTTCTTACTCTCACTAGTGGTAG-3′) and SS-R4-3 containing the *Hind*III site (5′-AAAGGGCCTAAGCTTGCCATGTCTAAGCTACCTATATTTATAATTATAA-3′). Using 2 plasmids encoding the SARS-CoV spike S1 protein-TW1-#19 (nt 21,826–22,087), the S1 protein and the S2 protein-TW1-#20 (nt 23,077–24,454) as templates, the S1-2 encoding SARS-CoV S protein 447–641 amino acid was produced and amplified by PCR, using one pair of primers: SS-F3-2 containing the *Hind*III site (5′-GACATGGCAAGCTTAGGCCCTTT-3′) and SS-R3 containing the *Sal*I site (5′-GAAGTGTCGACATGCTCAGCTC-3′). The PCR products of S1-1 and S1-2 were subsequently cloned into pGEX-6P-3 and pGEX-6P-1 (Amersham Biosciences, NJ, USA) through *Eco*RI/*Hind*III and *Hind*III/*Sal*I digestion and ligation, respectively. The S1-1 fragment was subcloned into S1-2/pGEX-6P-1 through *Eco*RI/*Hind*III digestion and ligation to form S1-3/pGEX-6P-1, using standardized molecular cloning technologies (Sambrook et al., 1989).

2.2. Protein expression and purification

The *Escherichia coli* culture was performed based on standard methods (Sambrook et al., 1989; Liou et al., 2011; Chang et al., 2012; Tseng et al., 2013). The glutathione-S transferase (GST)-containing recombinant protein expression plasmids S1-1/pGEX-6P-3, S1-2/pGEX-6P-1, S1-3/pGEX-6P-1, and pGEX-2KS (Chang et al., 1993, 2002) were transformed into the *E. coli* strain BL21 (DE3) for expression. The induction and purification of the recombinant proteins were performed using methods modified from previous studies (Chang et al., 1993, 1997b, 2000; Chang and Lo, 2000; Sun et al., 2007). Bacteria containing the expression plasmids were grown in a 2× YT broth (1.6% trypton, 1% yeast extract, and 0.5% NaCl) at 37 °C. The recombinant proteins were induced by adding isopropyl β-D-1-thiogalactopyranoside (IPTG) (1 mM) to the medium after the optical density (OD) of the bacterial culture reached 1.0. The optimal induction conditions were incubated at 37 °C for 2 h (S1-2/pGEX-6P-1, S1-3/pGEX-6P-1, and pGEX-2KS) and 4 h (S1-1/pGEX-6P-3). For purification, the centrifuged pellets of *E. coli* cells from a 1-L culture were resuspended in 50 mL 1× phosphate-buffered saline (PBS) containing protease inhibitors-1 mM phenylmethylsulfonyl fluoride (PMSF), 0.7 μg/mL of pepstatin, 1 μg/mL of leupeptin, and 2 mg/mL of lysozyme. The bacterial cells were subsequently disrupted using a French Press. The cell lysates were centrifuged at 10,000 × *g* for 30 min and passed through 0.45-μm filters to remove insoluble cell components. The filtered-cell lysates were loaded into a glutathione sepharose 4B column and the flow-through was again reloaded into the column to ensure saturated binding. The proteins were eluted using an elution buffer (10 mM glutathione; 50 mM Tris–HCl, pH 9.6; 1 mM PMSF; 0.7 μg/mL of pepstatin, and 1 μg/mL of leupeptin) and dialyzed with 1× PBS containing 1 mM PMSF. Consequently, all recombinant proteins used in this study were GST tagged. The protein concentration was determined using a protein assay kit (Bio-Rad, Hercules, CA, USA).

2.3. Antibody generation and purification

New Zealand rabbits were purchased from the National Laboratory Animal Center (Taipei, Taiwan) and maintained in a specific pathogen-free condition in the experimental animal center of Tzu Chi University. The research methods involving the experimental rabbits were performed under strict adherence to the guidelines of the Institutional Animal Care and Use Committee (Tzu Chi University) and the guidance of Animal Protection Law (Taiwan). Using methods modified from previous studies (Harlow and Lane, 1988; Chang et al., 2002; Sun et al., 2007), 250–500 μg of purified recombinant proteins were mixed with complete Freund's adjuvant and injected into New Zealand rabbits for the first immunization. For boosting, 100–250 μg proteins were mixed with incomplete Freund's adjuvant and injected in immunization cycles in 3-week intervals. After 5 immunizations, sera from rabbits were isolated and passed through the Protein A column. Immunoglobulin IgG fractions were eluted using an elution buffer (0.1 M citric acid, pH 3.0) and dialyzed with 1× PBS.

2.4. Synthetic peptides

Synthetic peptides GA91 (corresponding to SARS-CoV Spike protein 437–461 amino acids) were produced in linear form. Synthetic peptides GA101 (corresponding to SARS-CoV S protein 436–445 amino acids), GA107 (corresponding to SARS-CoV S protein 466–475 amino acids), and GA142 (corresponding to SARS-CoV S protein 100–109 amino acids) were produced in branched multiple antigenic peptide (M8) form. All synthetic peptides were provided by Genesis Biotech (Taipei, Taiwan).

2.5. Cell culture and cell-adhesion/inhibition assay

Vero E6 cells (ATCC No. C1008) and HeLa cells (ATCC No. CCL-2.2) were maintained in RPMI 1640 (BioWest, Miami, FL, USA), and NIH3T3 cells (ATCC No. CRL-1658) were maintained in Dulbecco's modified Eagle's medium (DMEM) (BioWest) containing 10% heat-inactivated fetal bovine serum (Biological Industries, Beit Haemek, Israel), 2 mM l-glutamine (BioWest), 100 U/L of penicillin (BioWest), 100 mg/mL of streptomycin (BioWest), and non-essential amino acid (BioWest). Cell adhesion and inhibition assays were performed according to our previously described methods (Chang et al., 1993, 1997a; Chang and Lo, 1998; Chang et al., 1999, 2001, 2002, 2003; Chang et al., 2005; Sun et al., 2005; Chang and Lo, 2007). Recombinant proteins (1.2 μg/30 μL/cover slip) were coated on cover slips at 37 °C for 1 h in 6-well microtiter plates, and then blocked with 5% bovine serum albumin (BSA) at 37 °C for a further hour. After being washed twice with PBS, cells (1×10^6) pre-mixed with antibodies (75 μg) or synthetic peptides (10 nmol) at 37 °C

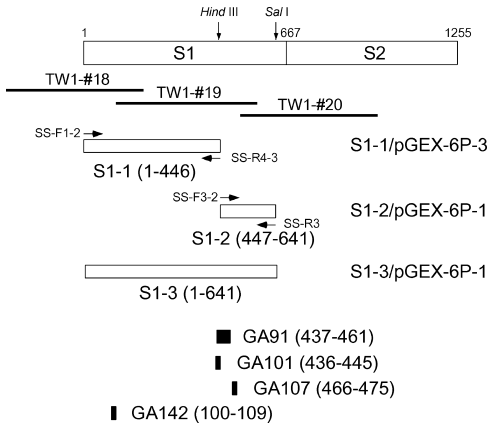

Fig. 1. Relative locations of SARS-CoV spike protein fragments S1-1 (1–446), S1-2 (447–641), and S1-3 (1–641) and related peptides. Using 3 plasmids encoding the SARS-CoV spike S1 and S2 proteins, TW1-#18, TW1-#19, and TW1-#20, as templates, S1-1 encoding the SARS-CoV S protein 1–446 amino acids and S1-2 encoding the SARS-CoV S protein 446–641 amino acids was produced and amplified using PCR, using 2 primers: SS-F1-2 and SS-R4-3, and SS-F3-2 and SS-R3, respectively. The PCR products of S1-1 and S1-2 were subcloned into pGEX-6P-3 and pGEX-6P-1 to form S1-1/pGEX-6P-3 and S1-2/pGEC-6P-1. The S1-1 fragment was subcloned into S1-2/pGEX-6P-1 to form S1-3/pGEX-6P-1. Synthetic peptides GA91 (spanning 437–461 amino acids of the SARS-CoV S protein), GA101 (spanning 436–445 amino acids of the SARS-CoV S protein), GA107 (spanning 466–475 amino acids of the SARS-CoV S protein), and GA142 (spanning 100–109 amino acids of the SARS-CoV S protein) are shown in the black boxes.

for 30 min were seeded onto pre-coated cover-slips and grown in medium at 37 °C for 45 min. After being washed twice with PBS, cells were fixed with 4% paraformaldehyde (in 1× PBS) at room temperature for 30 min. After being washed with PBS again, the cells were examined using an inverted microscope (Axiovert 40 CFL, Carl Zeiss, Gottingen, Germany) and photographed.

3. Results

3.1. Construction of expression plasmids for the SARS-CoV spike protein

The cell adhesion assay required recombinant proteins of the S1 domain and corresponding antibodies. Previous studies have reported that prokaryotic expressed non-glycosylated recombinant S proteins retained their function (Zhou et al., 2004; Chakraborti et al., 2005; Zhao et al., 2005). In this study, different fragments of the S1 domain (S1-1, S1-2, and S1-3) were constructed into *E. coli* expression vectors and expressed as glutathione *S*-transferase (GST)-fusion proteins (Fig. 1). S1-1 and S1-2 recombinant proteins, encompassing amino acids 1–446 and 447–641 of the S protein, were used to immunize rabbits for 5 immunization-cycles to obtain corresponding antibodies.

3.2. Determination of potential binding site of SARS-CoV spike proteins by using a cell adhesion assay

Previous studies have shown that SARS-CoV can infect the kidney cells of the African green monkey (Vero E6) (Li et al., 2003; Marra et al., 2003). Purified GST, S1-3, and S1-2 recombinant protein-coated cover slips and Vero E6 cells were used to perform a cell adhesion assay. The cell-adhesion efficiency of Vero-E6 cells to S1-3 coated cover slips were approximately 1.5 to 1.7-fold higher than that on GST-coated controls (Figs. 2A-a-b, B, 4A-a-b, and B). These results indicate that *E. coli*-derived S1-3 contains functional RBD for Vero E6 cells. In contrast, the efficiency of cell adhesion on S1-2 coated substrates is less than that of substrates coated with the control protein GST (Fig. 2A-c and B). The cell adhesion of Vero

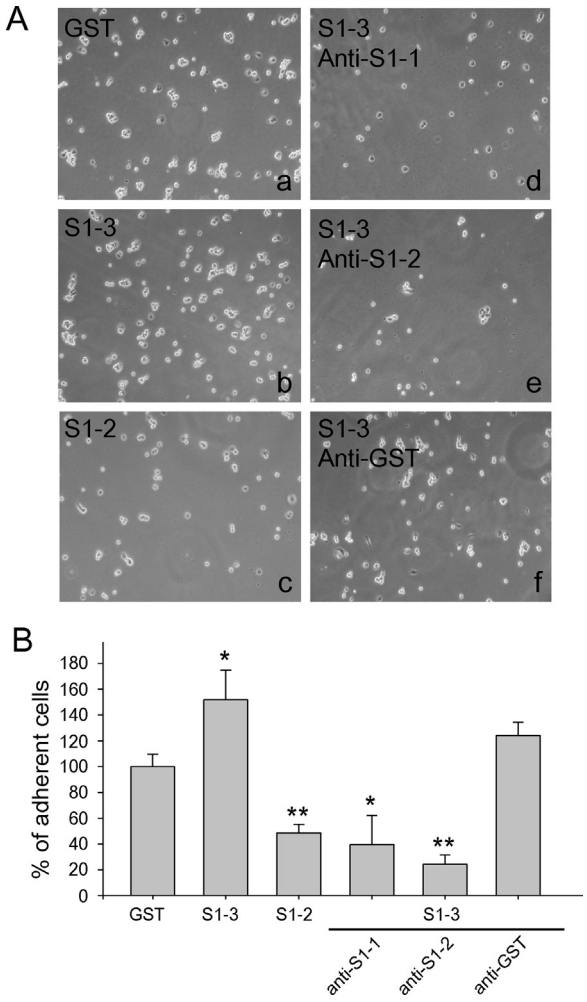

Fig. 2. The SARS-CoV S protein fragment S1-3 significantly accelerated the cell adhesion of Vero E6 cells and this effect can be inhibited by anti-S1-1 and anti-S1-2 antibodies. Recombinant proteins GST, S1-2, and S1-3 (1.2 μg) were coated on cover-slips in a 6-well dish, which was blocked with 5% bovine serum albumin. Vero E6 cells were seeded onto recombinant S protein-coated cover-slips and a binding assay was subsequently performed (A, a–c). For the inhibition assay, Vero E6 cells were pre-mixed with antibodies (75 μg) and seeded onto S1-3 pre-coated cover-slips (A, d–f). Cell images were captured using an inverted microscope at 100× magnification. The adherent cells were counted from 3 randomly selected (nonoverlapping) fields of each condition. The average cell counts of adherent cells in the GST-coated groups served as controls and defined as 100%. The percentages of adherent cells are shown in (B). $^{*}P < 0.05$, $^{**}P < 0.01$ compared with the control groups. Data are reported as the mean ± standard deviation (SD).

E6 on S1-3 coated substrates could be inhibited by rabbit polyclonal antibodies against S1-1 and S1-2, but cannot be inhibited by control antibodies against GST (Fig. 2A-d–f and B). These results indicated that the RBD potentially locates around the S1-1 and S1-2 junction region.

3.3. The permissive cell line Vero E6 but not the non-permissive cell lines HeLa and NIH 3T3 adhere to SARS-S coated surfaces

To verify whether the S protein-mediated cell adhesion is specific to SARS-CoV permissive cells (e.g., Vero E6 cells), 2 SARS-CoV nonpermissive cell lines, HeLa and NIH3T3 [which cannot be infected by SARS-CoV (Wang et al., 2004)], were used as controls to perform the cell adhesion assay. The cell-adhesion efficiency of NIH3T3 or HeLa cells to GST and S1-3 coated substrates did not show significant differences (Fig. 3). This suggests that

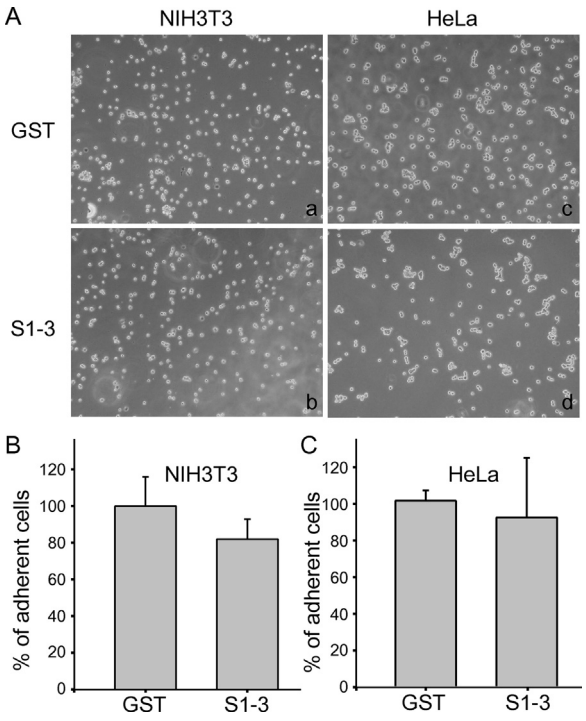

Fig. 3. SARS nonpermissive cell lines (NIH3T3 and HeLa) have no preferential cell adhesion to the GST-tagged SARS-CoV S protein fragment S1-3 when compared with the GST control protein. Recombinant proteins GST (A-a and A-c) and S1-3 (A-b and A-d) (1.2 μg) were coated on cover-slips in 6-well dishes. NIH3T3 (A, left panel) and HeLa cells (A, right panel) were seeded onto recombinant protein pre-coated cover-slips and performed binding assay. Cell images were captured using an inverted microscope at 100× magnification. The adherent cells were counted from 3 randomly selected (nonoverlapping) fields of each condition. The average cell counts of adherent cells in the GST-coated groups served as controls. The percentages of adherent cells of the NHI3T3 and HeLa cells groups are shown in (B) and (C), respectively. Data are reported as the mean ± SD.

S1-3-mediated cell adhesion can be specifically applied on SARS-CoV permissive cells.

3.4. The minimum binding site can be determined using peptides in the inhibition assay for cell adhesion

To narrow down the RBD of S protein, several synthetic peptides corresponding to the S1-1 and S1-2 junction region were used to perform the inhibition assay for cell adhesion. Our data revealed that synthetic peptides GA91 (spanning residues 437–461) and GA101 (spanning residues 436–445) inhibit the cell adhesion of Vero E6 cells on S1-3 coated substrates. GA107 (spanning residues 466–475) exerted a smaller inhibitory effect than GA91 and GA101 did in the cell binding assay. GA42 (spanning residues 100–109) encompassing amino acid residues outside the junction between S1-1 and S1-2 exerted only minor inhibition effects in the cell binding assay (Fig. 4).

4. Discussion

In this study, a simple, quick, and safe method was established to narrow down the RBM within the RBD of SARS-CoV S protein. Most popular methods investigating the RBD of SARS-CoV S identify fragments of SARS S protein binding to cells by using flow cytometry analysis (Babcock et al., 2004; He et al., 2004; Sui et al., 2004; Wong et al., 2004; Zhou et al., 2004) and an immunofluorescence assay (Chou et al., 2005; Ho et al., 2006), or determine the binding between ACE2 protein and S protein by using an enzyme-linked immunosorbent assay (ELISA) (Xiao et al., 2003; He et al., 2004; Ho et al., 2006). Although the cell adhesion assay developed in this study might not provide high quantitative and sensitive data that matches the flow cytometry (Babcock et al., 2004; He et al., 2004; Sui et al., 2004; Wong et al., 2004; Zhou et al., 2004) and ELISA-based analyses (Xiao et al., 2003; He et al., 2004; Ho et al., 2006), the analysis only requires recombinant proteins, peptides, virus permissive cells, and an ordinary light microscope to accomplish. Consequently, expensive equipment such as the flow cytometer, fluorescence microscope, and ELISA/fluorescence microplate readers are unnecessary, and this assay can be easily conducted in general laboratories, including those in third world countries. Because cell adhesion can be easily measured using MTT [3-(4,5-dimethylthiazol-2-yl)-2,5-diphenyltetrazolium bromide, a yellow tetrazole] assays, this method has the potential of being developed as a high throughput screening system for small molecule inhibitors when combined with automatic and robotic systems, which are unsuitable for flow cytometry and the immunofluorescence microscope based-assay. ELISA is also available for high throughput or fast screening systems; however, the recombinant ACE2 protein may not completely present as the native form of ACE2 on the surfaces of SARS-CoV permissive cells. ELISA-based analyses are only suitable to conduct after identifying the cellular receptor, for example after identifying ACE2; however, this study demonstrated that the novel cell-adhesion approach can be conducted even before identifying the cellular receptor.

For unknown reasons, the cell adhesion of Vero E6 cells to SARS-S (S1-2) substrates, which do not contain the RBD, with a lower efficiency than that of control protein GST (Fig. 2). The functional comparisons between different but related cell-adhesion proteins are difficult. For example, previously we found that even a single alanine insertion in various places around the cell-binding motif RGD (R: arginine; G: glycine; D: aspartic acid) of the snake-venom-protein rhodostomin could result a dramatically difference of cell-adhesion property. An alanine insertion at position 56 (between 56th and 57th amino acid of rhodostomin) could disrupt the cell-adhesion function of rhodostomin, while single insertions at positions 45–55 were not (Chang et al., 2001). Because the remaining protein backbone is unchanged in this case, these results suggest that the protein structure of rhodostomin is the key determinant of cell-adhesion function. Even though, the protein backbone may play an important role in other conditions. For example, evidences indicate that positive charge poly-amino acids such as poly-lysine can serve as a cell adhesion component (Mazia et al., 1975; Rajnicek et al., 1998; Brynda et al., 2005). In addition, net positive charge of cell-attached substratum seems to play a positive role on lamellipodia, filopodia formation, cell-adhesion and cell-growth (Rajnicek et al., 1998; Brynda et al., 2005). As a result, after analyzing the amino acid sequences of recombinant GST-S1-2 and GST proteins, which encoded by S1-2/pGEX-6P-1 and pGEX-2KS, respectively, we found that pGEX-2KS-encoded GST contains more positive-charge amino acids than S1-2/pGEXT-6P-1-encoded GST-S1-2 (GST: 13%; GST-S1-2: 10%). These phenomena, which include differences on the protein structures and positive changes, may explain the reason why cell adhesion to GST-substrates was more efficient than that of GST-S1-2-substrates. Nonetheless, further functional and structural investigations are needed to address the possibilities. Despite of this, the assay in our condition has a great resolution power (with high reproducibility and significantly) to distinguish the levels of cell adhesion when RBD-containing proteins were used. This suggests that the analysis system has great potentials on the analysis of RBD of viral proteins.

Using this method, our data suggest that peptides spanning residues 436–445 and 437–461 of the S protein are the minimal size of peptides to block the binding of the SARS-CoV S protein to Vero-E6 cells. These peptides are located within the hundred-amino-acids RBDs previously identified using other methods (Xiao et al., 2003; Babcock et al., 2004; He et al., 2004; Sui et al., 2004;

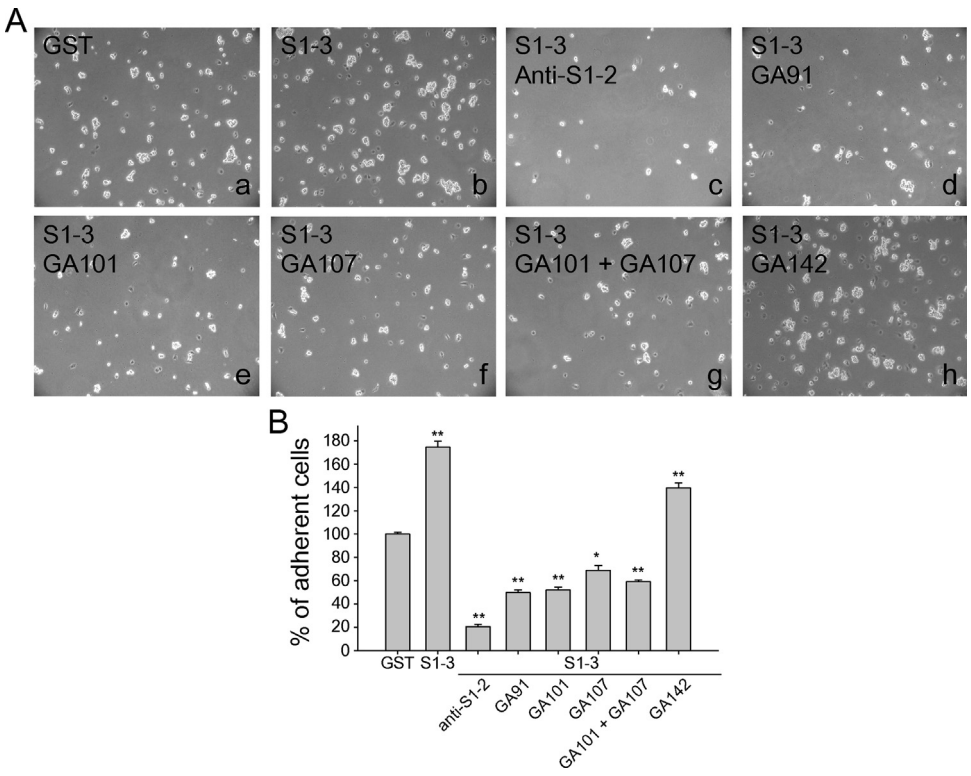

Fig. 4. The SARS-CoV S protein fragment S1-3-mediated cell adhesion can be inhibited by peptides within the receptor binding domain. Recombinant proteins S1-3 (A, b–h) (1.2 μg) were coated on cover-slips in a 6-well dish. Vero E6 cells were pre-mixed with 75 μg of anti-S1-2 antibodies, 10 nmol synthetic peptides GA91 (A–d), GA101 (A–e), GA107 (A–f), GA101 + GA107 (A–g), and GA142 (A–h) and seeded onto S1-3 pre-coated cover-slips to perform the binding inhibition assay. Cell images were captured using an inverted microscope at 100× magnification. The adherent cells were counted from 3 randomly selected (nonoverlapping) fields of each condition. The average cell counts of adherent cells in the GST-coated groups served as controls. The percentages of adherent cells are shown in (B). $^{*}P < 0.05$, $^{**}P < 0.01$ compared with the control groups. Data are reported as the mean ± SD.

Wong et al., 2004) and are within the RBM (residues 424–494) characterized by the crystal structure of the SARS-CoV S protein (residues 306–527) and the ACE2 complex (Li et al., 2005). These peptides also overlap with a hexapeptide (residues 438–443), which blocks viral entry into host cells through ACE2 (Struck et al., 2012). These peptides cover most parts of the putative high antigenicity site (residues 426–456) reported by the Hsiang CY group (Ho et al., 2004). These peptides are useful as peptide inhibitors and are optimal candidates for developing the SARS peptide vaccine.

Acknowledgments

This work was supported by grants from Tzu-Chi University (TCMRC9220). The authors are grateful to Professor Chen PJ (National Taiwan University, Hepatitis Research Center) for generously providing SARS-CoV spike-gene containing plasmids TW1-#18, TW1-#19, and TW1-#20. We also greatly appreciate Genesis Biotech (Taipei, Taiwan) for kindly providing all synthetic peptides. The authors also want to thank Professor Wang MH and his team (Experimental Animal Center, Tzu-Chi University) for their help in maintaining the experimental animals and the pathogen-free environments. We deeply appreciate Professor Chen JH (Department of Molecular Biology and Human Genetics, Tzu-Chi University), Professor Pang CY (Institute of Medical Sciences, Tzu-Chi University), and Professor Lo SY (Department of Laboratory Medicine and Technology, Tzu-Chi University) for kindly providing HeLa, NIH3T3, and the Vero E6 cell lines, respectively.

References

Babcock, G.J., Esshaki, D.J., Thomas Jr., W.D., Ambrosino, D.M., 2004. Amino acids 270 to 510 of the severe acute respiratory syndrome coronavirus spike protein are required for interaction with receptor. J. Virol. 78, 4552–4560.

Brynda, E., Pachernik, J., Houska, M., Pientka, Z., Dvorak, P., 2005. Surface immobilized protein multilayers for cell seeding. Langmuir 21, 7877–7883.

Chakraborti, S., Prabakaran, P., Xiao, X., Dimitrov, D.S., 2005. The SARS coronavirus S glycoprotein receptor binding domain: fine mapping and functional characterization. Virol. J. 2, 73.

Chang, C.P., Chang, J.C., Chang, H.H., Tsai, W.J., Lo, S.J., 2001. Positional importance of Pro53 adjacent to the Arg49-Gly50-Asp51 sequence of rhodostomin in binding to integrin alphaIIbbeta3. Biochem. J. 357, 57–64.

Chang, H.H., Chang, C.P., Chang, J.C., Dung, S.Z., Lo, S.J., 1997a. Application of recombinant rhodostomin in studying cell adhesion. J. Biomed. Sci. 4, 235–243.

Chang, H.H., Hu, S.T., Huang, T.F., Chen, S.H., Lee, Y.H., Lo, S.J., 1993. Rhodostomin, an RGD-containing peptide expressed from a synthetic gene in *Escherichia coli*, facilitates the attachment of human hepatoma cells. Biochem. Biophys. Res. Commun. 190, 242–249.

Chang, H.H., Kau, J.H., Lo, S.J., Sun, D.S., 2003. Cell-adhesion and morphological changes are not sufficient to support anchorage-dependent cell growth via non-integrin-mediated attachment. Cell Biol. Int. 27, 123–133.

Chang, H.H., Lin, C.H., Lo, S.J., 1999. Recombinant rhodostomin substrates induce transformation and active calcium oscillation in human platelets. Exp. Cell Res. 250, 387–400.

Chang, H.H., Lo, S.J., 1998. Full-spreading platelets induced by the recombinant rhodostomin are via binding to integrins and correlated with FAK phosphorylation. Toxicon 36, 1087–1099.

Chang, H.H., Lo, S.J., 2000. Modification with a phosphorylation tag of PKA in the TraT-based display vector of *Escherichia coli*. J. Biotechnol. 78, 115–122.

Chang, H.H., Lo, S.J., 2007. Snake venom disintegrin rhodostomin served as a molecular tool to dissect the integrin function. Toxin Rev. 26, 189–202.

Chang, H.H., Shih, K.N., Lo, S.J., 2000. Receptor-mediated endocytosis as a selection force to enrich bacteria expressing rhodostomin on their surface. J. Biomed. Sci. 7, 42–50.

Chang, H.H., Shyu, H.F., Wang, Y.M., Sun, D.S., Shyu, R.H., Tang, S.S., Huang, Y.S., 2002. Facilitation of cell adhesion by immobilized dengue viral nonstructural protein 1 (NS1): arginine-glycine-aspartic acid structural mimicry within the dengue viral NS1 antigen. J. Infect. Dis. 186, 743–751.

Chang, H.H., Tsai, W.J., Lo, S.J., 1997b. Glutathione S-transferase-rhodostomin fusion protein inhibits platelet aggregation and induces platelet shape change. Toxicon 35, 195–204.

Chang, J.C., Chang, H.H., Lin, C.T., Lo, S.J., 2005. The integrin alpha6beta1 modulation of PI3K and Cdc42 activities induces dynamic filopodium formation in human platelets. J. Biomed. Sci. 12, 881–898.

Chang, W.K., Sun, D.S., Chan, H., Huang, P.T., Wu, W.S., Lin, C.H., Tseng, Y.H., Cheng, Y.H., Tseng, C.C., Chang, H.H., 2012. Visible light-responsive core-shell structured In2O3@CaIn2O4 photocatalyst with superior bactericidal properties and biocompatibility. Nanomedicine 8, 609–617.

Chou, C.F., Shen, S., Tan, Y.J., Fielding, B.C., Tan, T.H., Fu, J., Xu, Q., Lim, S.G., Hong, W., 2005. A novel cell-based binding assay system reconstituting interaction between SARS-CoV S protein and its cellular receptor. J. Virol. Methods 123, 41–48.

Drosten, C., Gunther, S., Preiser, W., van der Werf, S., Brodt, H.R., Becker, S., Rabenau, H., Panning, M., Kolesnikova, L., Fouchier, R.A., Berger, A., Burguiere, A.M., Cinatl, J., Eickmann, M., Escriou, N., Grywna, K., Kramme, S., Manuguerra, J.C., Muller, S., Rickerts, V., Sturmer, M., Vieth, S., Klenk, H.D., Osterhaus, A.D., Schmitz, H., Doerr, H.W., 2003. Identification of a novel coronavirus in patients with severe acute respiratory syndrome. N. Engl. J. Med. 348, 1967–1976.

Gallagher, T.M., Buchmeier, M.J., 2001. Coronavirus spike proteins in viral entry and pathogenesis. Virology 279, 371–374.

Harlow, E., Lane, D., 1988. Antibodies: A Laboratory Manual. Cold Spring Harbor Laboratory, New York.

He, Y., Zhou, Y., Liu, S., Kou, Z., Li, W., Farzan, M., Jiang, S., 2004. Receptor-binding domain of SARS-CoV spike protein induces highly potent neutralizing antibodies: implication for developing subunit vaccine. Biochem. Biophys. Res. Commun. 324, 773–781.

Ho, T.Y., Wu, S.L., Chen, J.C., Wei, Y.C., Cheng, S.E., Chang, Y.H., Liu, H.J., Hsiang, C.Y., 2006. Design and biological activities of novel inhibitory peptides for SARS-CoV spike protein and angiotensin-converting enzyme 2 interaction. Antiviral Res. 69, 70–76.

Ho, T.Y., Wu, S.L., Cheng, S.E., Wei, Y.C., Huang, S.P., Hsiang, C.Y., 2004. Antigenicity and receptor-binding ability of recombinant SARS coronavirus spike protein. Biochem. Biophys. Res. Commun. 313, 938–947.

Holmes, K.V., 2003. SARS-associated coronavirus. N. Engl. J. Med. 348, 1948–1951.

Jiang, S., Lu, L., Du, L., 2013. Development of SARS vaccines and therapeutics is still needed. Future Virol. 8, 1–2.

Kuehn, B.M., 2013. Lessons learned from SARS outbreak prompt rapid response to new coronavirus. JAMA 309, 1576–1577.

Li, F., Li, W., Farzan, M., Harrison, S.C., 2005. Structure of SARS coronavirus spike receptor-binding domain complexed with receptor. Science 309, 1864–1868.

Li, W., Moore, M.J., Vasilieva, N., Sui, J., Wong, S.K., Berne, M.A., Somasundaran, M., Sullivan, J.L., Luzuriaga, K., Greenough, T.C., Choe, H., Farzan, M., 2003. Angiotensin-converting enzyme 2 is a functional receptor for the SARS coronavirus. Nature 426, 450–454.

Liou, J.W., Gu, M.H., Chen, Y.K., Chen, W.Y., Chen, Y.C., Tseng, Y.H., Hung, Y.J., Chang, H.H., 2011. Visible light responsive photocatalyst induces progressive and apical-terminus preferential damages on *Escherichia coli* surfaces. PLoS One 6, e19982.

Marra, M.A., Jones, S.J., Astell, C.R., Holt, R.A., Brooks-Wilson, A., Butterfield, Y.S., Khattra, J., Asano, J.K., Barber, S.A., Chan, S.Y., Cloutier, A., Coughlin, S.M., Freeman, D., Girn, N., Griffith, O.L., Leach, S.R., Mayo, M., McDonald, H., Montgomery, S.B., Pandoh, P.K., Petrescu, A.S., Robertson, A.G., Schein, J.E., Siddiqui, A., Smailus, D.E., Stott, J.M., Yang, G.S., Plummer, F., Andonov, A., Artsob, H., Bastien, N., Bernard, K., Booth, T.F., Bowness, D., Czub, M., Drebot, M., Fernando, L., Flick, R., Garbutt, M., Gray, M., Grolla, A., Jones, S., Feldmann, H., Meyers, A., Kabani, A., Li, Y., Normand, S., Stroher, U., Tipples, G.A., Tyler, S., Vogrig, R., Ward, D., Watson, B., Brunham, R.C., Krajden, M., Petric, M., Skowronski, D.M., Upton, C., Roper, R.L., 2003. The genome sequence of the SARS-associated coronavirus. Science 300, 1399–1404.

Matsuyama, S., Taguchi, F., 2002. Receptor-induced conformational changes of murine coronavirus spike protein. J. Virol. 76, 11819–11826.

Mazia, D., Schatten, G., Sale, W., 1975. Adhesion of cells to surfaces coated with polylysine. Applications to electron microscopy. J. Cell Biol. 66, 198–200.

Peiris, J.S., Lai, S.T., Poon, L.L., Guan, Y., Yam, L.Y., Lim, W., Nicholls, J., Yee, W.K., Yan, W.W., Cheung, M.T., Cheng, V.C., Chan, K.H., Tsang, D.N., Yung, R.W., Ng, T.K., Yuen, K.Y., group, S.s., 2003. Coronavirus as a possible cause of severe acute respiratory syndrome. Lancet 361, 1319–1325.

Rajnicek, A.M., Robinson, K.R., McCaig, C.D., 1998. The direction of neurite growth in a weak DC electric field depends on the substratum: contributions of adhesivity and net surface charge. Dev. Biol. 203, 412–423.

Ruan, Y.J., Wei, C.L., Ee, A.L., Vega, V.B., Thoreau, H., Su, S.T., Chia, J.M., Ng, P., Chiu, K.P., Lim, L., Zhang, T., Peng, C.K., Lin, E.O., Lee, N.M., Yee, S.L., Ng, L.F., Chee, R.E., Stanton, L.W., Long, P.M., Liu, E.T., 2003. Comparative full-length genome sequence analysis of 14 SARS coronavirus isolates and common mutations associated with putative origins of infection. Lancet 361, 1779–1785.

Sambrook, J., Fritsch, E.F., Maniatis, T., 1989. Molecular Cloning: A Laboratory Manual, 2nd ed. Cold Spring Harbor Laboratory Press, Cold Spring Harbor, NY.

Struck, A.W., Axmann, M., Pfefferle, S., Drosten, C., Meyer, B., 2012. A hexapeptide of the receptor-binding domain of SARS corona virus spike protein blocks viral entry into host cells via the human receptor ACE2. Antiviral Res. 94, 288–296.

Sui, J., Li, W., Murakami, A., Tamin, A., Matthews, L.J., Wong, S.K., Moore, M.J., Tallarico, A.S., Olurinde, M., Choe, H., Anderson, L.J., Bellini, W.J., Farzan, M., Marasco, W.A., 2004. Potent neutralization of severe acute respiratory syndrome (SARS) coronavirus by a human mAb to S1 protein that blocks receptor association. Proc. Natl. Acad. Sci. U S A 101, 2536–2541.

Sun, D.S., King, C.C., Huang, H.S., Shih, Y.L., Lee, C.C., Tsai, W.J., Yu, C.C., Chang, H.H., 2007. Antiplatelet autoantibodies elicited by dengue virus non-structural protein 1 cause thrombocytopenia and mortality in mice. J. Thromb. Haemost. 5, 2291–2299.

Sun, D.S., Lo, S.J., Tsai, W.J., Lin, C.H., Yu, M.S., Chen, Y.F., Chang, H.H., 2005. PI3-kinase is essential for ADP-stimulated integrin alpha(IIb)beta3-mediated platelet calcium oscillation, implications for P2Y receptor pathways in integrin alpha(IIb)beta3-initiated signaling cross-talks. J. Biomed. Sci. 12, 937–948.

Tseng, Y.H., Sun, D.S., Wu, W.S., Chan, H., Syue, M.S., Ho, H.C., Chang, H.H., 2013. Antibacterial performance of nanoscaled visible-light responsive platinum-containing titania photocatalyst in vitro and in vivo. Biochim. Biophys. Acta 1830, 3787–3795.

Wang, P., Chen, J., Zheng, A., Nie, Y., Shi, X., Wang, W., Wang, G., Luo, M., Liu, H., Tan, L., Song, X., Wang, Z., Yin, X., Qu, X., Wang, X., Qing, T., Ding, M., Deng, H., 2004. Expression cloning of functional receptor used by SARS coronavirus. Biochem. Biophys. Res. Commun. 315, 439–444.

Wong, S.K., Li, W., Moore, M.J., Choe, H., Farzan, M., 2004. A 193-amino acid fragment of the SARS coronavirus S protein efficiently binds angiotensin-converting enzyme 2. J. Biol. Chem. 279, 3197–3201.

Wu, Y., Gao, G.F., 2013. Compiling of comprehensive data of human infections with novel influenza A (H7N9) virus. Front. Med. 7, 275–276.

Xiao, X., Chakraborti, S., Dimitrov, A.S., Gramatikoff, K., Dimitrov, D.S., 2003. The SARS-CoV S glycoprotein: expression and functional characterization. Biochem. Biophys. Res. Commun. 312, 1159–1164.

Zhao, J.C., Zhao, Z.D., Wang, W., Gao, X.M., 2005. Prokaryotic expression, refolding, and purification of fragment 450–650 of the spike protein of SARS-coronavirus. Protein Expr. Purif. 39, 169–174.

Zhou, T., Wang, H., Luo, D., Rowe, T., Wang, Z., Hogan, R.J., Qiu, S., Bunzel, R.J., Huang, G., Mishra, V., Voss, T.G., Kimberly, R., Luo, M., 2004. An exposed domain in the severe acute respiratory syndrome coronavirus spike protein induces neutralizing antibodies. J. Virol. 78, 7217–7226.